9781945541193/2017

MODULAR REAL-TIME SPECTROSCOPY INSTRUMENT

Ryan Striker[1], Andrew Vetter[1], Christopher Weberg[2], Stacy Staab[2], Branden Kaste[3], Meredith Schroeder[4], Raquib Hasan[5], Jordan Nodland[1], Amanda E. Brooks[5], Ben D. Brooks[1], Daniel L. Ewert[1]

[1]Department of Electrical and Computer Engineering
[2]Department of Mechanical Engineering
[3]Materials and Nanotechnology Program
[4]Department of Microbiology
[5]Department of Pharmaceutical Sciences
North Dakota State University
Fargo, ND, 58102

ABSTRACT

Whether researching new antibiotics, cancer treatments, or biofilm inhibitors, spectroscopy affords unique insight into nanoscale biochemical processes. Spectroscopy allows both the quantification and characterization of proteins, enzymes, DNA, and bacteria. Existing lab devices contain advanced optical systems which support selection of wavelengths. However, shortcomings of present equipment include high cost, the assumption of an on-site operator at each measurement interval, and limited sensitivity under particular circumstances. Furthermore, existing optical systems are incompatible with hybrid experimental arrangements such as automated fluid exchange or sample exposure to electromagnetic fields. A modular spectroscopy system is presented, centered around the popular Raspberry Pi single-board computer, which may be configured for multiple spectroscopy readings, including absorbance and fluorescence. Data collection on the Raspberry Pi is superior to existing systems because readings are automatically taken at a programmable interval, and the results are remotely available in real time. Mechanical flexibility is achieved by housing the sample cuvette in a 3D printed plastic block. Electromagnetic energy easily passes through the plastic material to reach the sample, and optoelectronics or fluidics may access the cuvette through identical ports on each of the block's six faces. Finally, the block can be modified and reprinted in a single day if new features are desired. The modular ports enable quantifiable interdisciplinary experiments such as real-time measurement of both drug concentration and bacterial inhibition; researchers may monitor a drug's release kinetics from a polymer matrix (absorbance) while also measuring the drug's inhibitory effect on bacterial growth (fluorescence).

Keywords: spectroscopy, absorbance, fluorescence, dissolution

INTRODUCTION

This paper presents a work-in-progress update on the development of a modular real-time spectroscopy system. As shown in Figure 1, this spectroscopy system differs from existing lab instruments as the entire experimental reaction may be conducted within the device. That is, spectroscopic measurement of an experiment's moment-by-moment progress does not require a pause or halt to the experiment; sensitive solutions do not need to be pipetted between vessels, and fragile cuvettes do not need to be lifted in/out of racks. By both reducing and simplifying the optical and electronic components traditionally

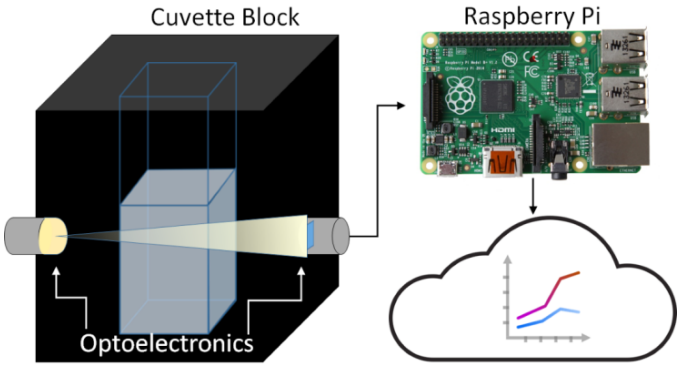

Figure 1 – The principle elements of the RTSpec system are a cuvette block, optoelectronics, and a Raspberry Pi computer. Measured data is pushed to a publicly accessible web server for remote viewing and plotting.

placed in close proximity to the cuvette, new features such as fluid flow, RF antennas/coils, and additional optical sensors may be added.

A generation one system with the ability to accurately measure 280 nm absorbance was previously reported [1]. This paper presents subsequent updates to the system's software, electronics, and mechanicals. Motivations for recent updates include: smaller and more robust electronics which can be deployed to a lab and used by non-engineers without frequent repair or recalibration, the ability to measure fluorescence in addition to absorbance, and the ability to view experimental data remotely.

METHODS

To make experimental data available remotely, the web and data management tools of the burgeoning IoT (Internet of Things) industry were leveraged. Exosite was selected as the data portal/platform because of their support for graphical data visualization, a C code API library for the Raspberry Pi, and free service. Because the Raspberry Pi pushes data out to a web server, instead of accepting or processing inbound traffic, this architecture complies with most institutional network access policies and does not create an undue vulnerability to hacking.

PCBs (Printed Circuit Boards) were designed using freely available KiCAD schematic and PCB software. PCBs were fabricated by OSH Park, and electronic components were purchased from Digikey. Final assembly and test were performed by the research team. Solid models were designed in SolidWorks. 3D printing was performed on a FormLabs Form 1+ SLA with black resin.

RESULTS

Beyond simply collecting data at regular intervals, a key desire for pharmaceutical studies is maintaining the sink condition; this means that the concentration of a drug being dissolved into a buffer is significantly below its saturation point. When the concentration rises above a predetermined threshold, it is a relatively quick and straightforward procedure to remove and replace the buffer solution. However, because pharmacokinetic dissolution experiments are run over an extended duration from hours to months, researchers must remain in the lab for long and odd hours in order to monitor and maintain sink conditions and produce *in vivo* relevant data. A system which allows researchers to remotely monitor drug concentration would alleviate this time-intensive aspect. Instead of being forced to remain in the lab, researchers could instead monitor the concentration via a website accessible from their home or mobile device. Thus, changing the nature of the experiment from an arbitrary, investigator predetermined buffer exchange time point to a more relevant system determined time point.

Previously published data was collected using breadboard electronics. Such systems are useful for rapid experimentation and modification because power and signal wires can be easily unplugged, moved, and re-inserted. But, breadboard systems are also vulnerable to inadvertently disconnected wires, increased parasitic elements, and electromagnetic interference. The fragility of this arrangement necessitated an improved design; custom PCBs, which made the system more reliable and also more compact, were created. Once the new PCBs were assembled and tested, output sensor drift of >60% over 3 days was

observed. This instability was attacked in several ways: by reducing EMI sources, increasing power supply bulk capacitance, and reducing power supply path loss.
The I2C communication bus, which reports measurements to the Raspberry Pi computer, was considered a potential source of interference because transients were observed on the power supply at an identical time interval as the I2C communication. Therefore, the I2C pull-up resistance was increased from 5k to 10k ohms. After this change, no overshoot was observed on the lines and the rise times remained within the I2C specification. After applying this change, power supply transients were reduced but the large-scale drift issue remained.

The sensor PCB already contained several ceramic capacitors of 10 uF and below. It was hypothesized that high-frequency capacitance was adequate but bulk capacitance was lacking. Therefore, a 470 uF tantalum capacitor was added to the sensor PCB. After installing this component, sensor drift was reduced by a full order of magnitude. Total sensor drift is now <6%, and most of this occurs within an hour of applying power to the system. By “warming up” the system for one hour before collecting data, results can now be trusted as accurate to within 3% of full-scale.

In the course of investigating sensor drift, it was also observed that either poor orientation or slight angular displacement of connector wires could create measurement variations of >5%. To address this, the team changed all connectors from simple prototyping jumper wires to the Molex C-Grid III family of connectors which are both keyed (polarized) and locking. This change has worked as desired; measurements no longer fluctuate when cables are bumped, and correct cable insertion is enforced by the keyed connectors. With careful installation, these larger connectors were successfully installed onto the existing PCBs.

Electromechanical issues were also observed at the interface between the cuvette block and the input/output PCBs. The original aluminum block relied upon small set screws which impinged upon the outer metal can of the LED and photodiode components. This posed several challenges: electrical short circuits were created by the metal block, the set screws were crushing the LED and photodiode cans, and any torque upon the LED or photodiode cable assemblies was transferred to and concentrated on the LED and photodiode component leads. In short, the most critical components of the generation one spectroscopy system (the light source and light detector) were not adequately protected. The change from an aluminum block to a 3D printed plastic block quickly eliminated the short-circuit concerns. To eliminate the crushing effects of set-screws and also prevent cable strain from cracking solder joints, future iterations of the PCBs and the cuvette block will incorporate a hole pattern for mounting screws. Securing the PCBs to the cuvette block directly will better protect sensitive optical components and improve reliability and sensitivity.

Mechanically, the system centers on the cuvette block, which houses a standard 10 mm square cuvette. The block’s principal function is to block all ambient light so that spectroscopic measurements are not influenced by the surrounding environment. Additionally, the interior surfaces of the cuvette block should minimize optical reflection. The exterior of the cuvette block supports the attachment of optoelectronic input and output components; light passes directly through the cuvette via the red holes shown in Figure 2.

Previously, a machined aluminum cuvette block was used. This effectively blocked ambient light, but it was not an ideal solution. First, the design and fabrication of the block required staff and shop facilities outside the research group; this led to slower turnaround and higher cost for each design iteration. Next, as previously noted, short-circuiting of the optoelectronics was a concern. Finally, future experimental arrangements call for exposing the cuvette to RF energy which would be blocked or distorted by aluminum. For these reasons, the feasibility of a 3D printed cuvette block was explored via both Stereolithography (SLA) and Fused Filament Fabrication (extrusion). Ultimately, extrusion printing was not selected for this project because small voids between adjacent print lines and layers were observed. These voids had the potential to allow ambient light to reach the cuvette and corrupt spectroscopic measurements. Cuvette blocks were printed in a vertical orientation; this orientation confines defects resulting from build supports to the exterior of the block where tight dimensional tolerance is not required.

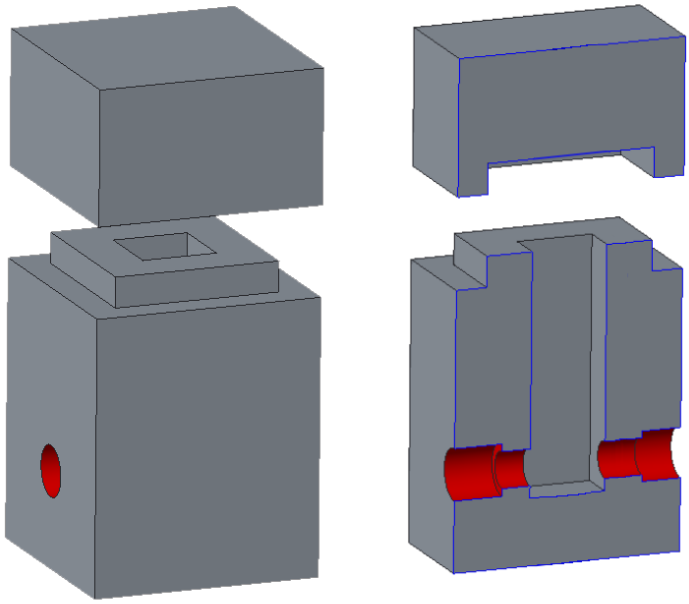

Figure 2 – The cuvette block is shown in exploded and cutaway views. The block consists two parts: a base and a lid. A 10 mm square cuvette is lowered into the block's center cavity and the lid applied. The block prevents ambient light from reaching the cuvette, and it supports/aligns the optoelectronic elements on the exterior.

Measuring fluorescence presented a unique set of technical challenges not encountered when measuring absorbance. Whereas absorbance uses the same wavelength of light at the system's input and output, fluorescence inputs one wavelength (excitation) and measures another (emission)[2], [3]. This is a challenge because output sensors (photodiodes) are typically broadband devices which respond to many wavelengths. That is, the photodiode would detect both the excitation and emission wavelengths. Without additional design measures, the photodiode's measurement would be so saturated by the excitation light that it would be unable to detect either the presence or the magnitude of fluorescent emission. To reject 485 nm excitation light and only measure fluorescently emitted light at 520 nm, a dichroic filter was added in front of the photodiode[4]. As shown in Figure 3, the dichroic filter is inserted via a top-loading slot in the cuvette block and rests in the optical path, between the photodiode and the cuvette.

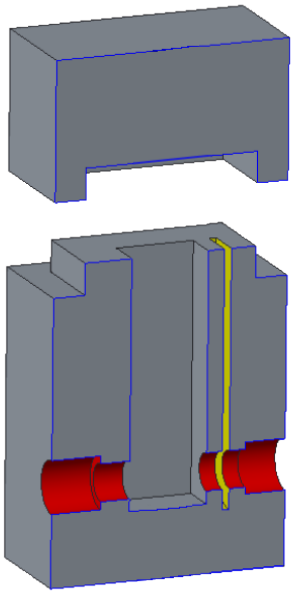

Figure 3 – A dichroic filter may be inserted between the cuvette and the photodiode sensor. This filter blocks the 485 nm excitation light but allows 520 nm emission light (fluorescence) to reach the photodiode sensor.

With the fundamentals of measuring fluorescence resolved, the simultaneous measurement of fluorescence and absorbance was addressed. This required additional orthogonal mounting sites for additional input/output sensor pairs. As seen in Figure 4 – To collect multiple measurements simultaneously, additional axes of the cuvette block are exploited. By adding a hole feature to each of the six block faces, three orthogonal input/output measurement paths are available.Figure 4, the cuvette block's six faces afford three distinct input/output paths. It is hypothesized that fluorescent measurement of biofilm growth will be most effective in the vertical (blue) axis, but this has not yet been experimentally tested.

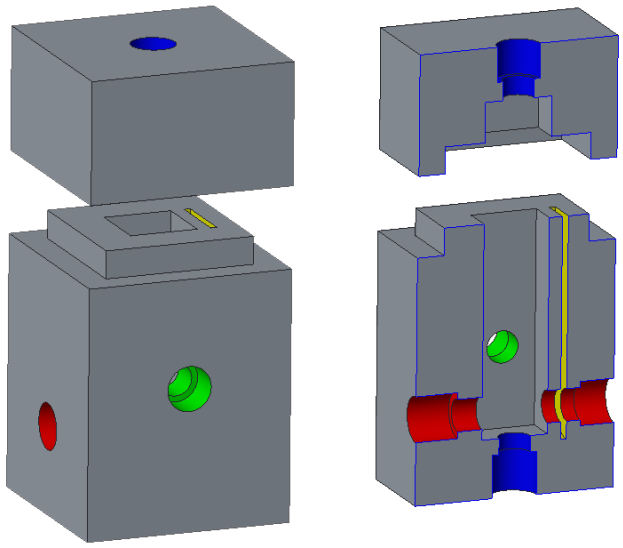

Figure 4 – To collect multiple measurements simultaneously, additional axes of the cuvette block are exploited. By adding a hole feature to each of the six block faces, three orthogonal input/output measurement paths are available.

It should also be noted that different measurements are not simultaneous in every sense of the word. They are spatially simultaneous in the sense that the sample need not be moved from one instrument to another. But, with respect to time, only one input/output system is active at a time. However, the time required to switch between measurement systems (<1 second) is miniscule when compared to the reaction rates of drug dissolution or biofilm growth (minutes/hours). Therefore, the measurements are effectively simultaneous for the experiments presently under consideration.

DISCUSSION

After many changes to the mechanical and electrical systems surrounding the cuvette, a verification step was conducted to collect absorbance readings of a serially diluted standard curve of vancomycin at 280 nm (Figure 5). The useful dynamic range is presently small, because only linear measurement regions may be used for pharmacokinetics. The linear range will be increased through the modification of electronic feedback and amplification values as well as the implementation of a software data filter on the Raspberry Pi.

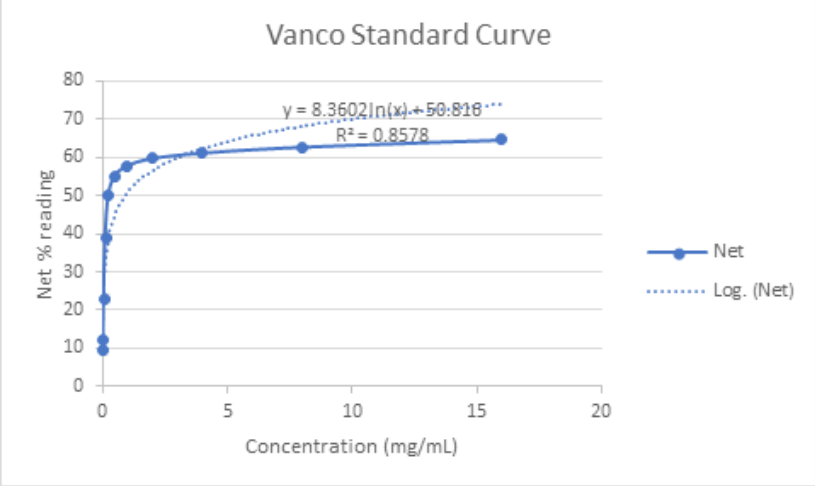

Figure 5 – Non-linear transmissivity (%) vs. concentration is shown for a serially diluted solution of Vancomycin.

9781945541193/2017

CONCLUSIONS

With the improvements described in this paper, the revised RTSpec system (Figure 6) is now sufficiently compact, accurate, and robust to be deployed into a pharmaceutical lab for regular use beyond the supervision/maintenance of the engineering team. This use will generate additional feedback regarding the system's ruggedness, reliability, and usability. Meanwhile, the engineering group will continue to develop and test additional features and improvements.

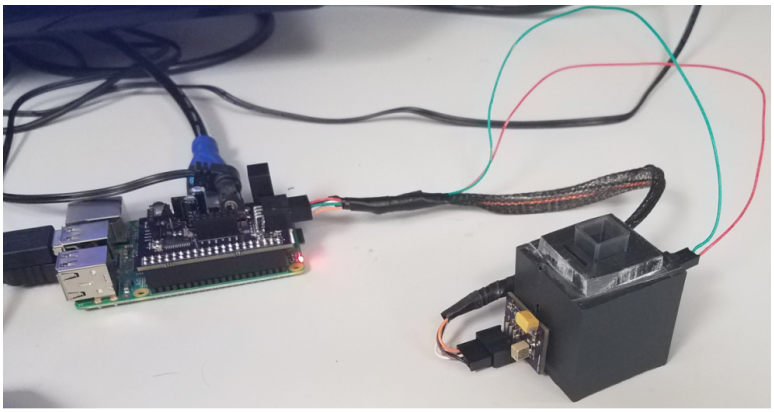

Figure 6 – The RTSpec system is shown. The Raspberry Pi is on the left. The 3D printed cuvette block is on the right. The lid is not in place, and a 10 mm cuvette can be seen protruding from the block.

In the future, all custom PCBs will be revised based upon recent debugging experience. Improvements include the addition of mounting holes, a shift to locking connectors, and locating voltage regulators closer to sensitive analog circuits.

Additional advancements will add a fluid exchange feature, allowing the system to autonomously monitor and maintain a sink condition throughout an extended dissolution experiment. Fluid exchange may be continuous, or it may be triggered at preset time intervals, or it may be initiated when the drug concentration crosses a preset threshold. Further refinements will also expand system capabilities to include measuring absorbance at 260 nm for monitoring dehybridization of DNA hairpin loops.

ACKNOWLEDGMENTS

This research was conducted as a part of an interdisciplinary, discovery-based learning (DBL) course sequence supervised by Drs. Daniel Ewert and Amanda Brooks; thank you to all students enrolled in this course for their insights, encouragement, and feedback. Additional thanks to Mary Pearson, Daniel Asa, Jared Hansen, and Jeffrey Erickson. Materials were purchased through Dr. A. Brooks's startup package from the NDSU Department of Pharmaceutical Sciences.

REFERENCES

[1] M. R. Hasan, J. Nodland, and A. E. Brooks, "A microfluidic platform for continuous monitoring of drug release kinetics," *Biomed Sci Instrum*, vol. 52, 2016.

[2] D. C. Prasher, V. K. Eckenrode, W. W. Ward, F. G. Prendergast, and M. J. Cormier, "Primary structure of the Aequorea victoria green-fluorescent protein," *Gene*, vol. 111, no. 2, pp. 229–233, Feb. 1992.

[3] "Excitation and Emission of Green Fluorescent Proteins." [Online]. Available: http://www.biotek.com/resources/articles/green-fluorescent-proteins.html. [Accessed: 06-Jan-2017].

[4] K. O. (UK) LTD, "Dichroic filter, longpass, 510nm, dia 12.5mm." [Online]. Available: https://www.knightoptical.com/stock/optical-components/uvvisnir-optics/filters/dichroic-filters/dichroic-longpass-filters/dichroic-filter-longpass-510nm-dia-125mm/. [Accessed: 06-Jan-2017].